HHS Public Access

Author manuscript

Alcohol Clin Exp Res. Author manuscript; available in PMC 2021 May 01.

Published in final edited form as:

Alcohol Clin Exp Res. 2020 May ; 44(5): 1046–1060. doi:10.1111/acer.14326.

Dihydromyricetin protects the liver via changes in lipid metabolism and enhanced ethanol metabolism

Joshua Silva[a], **Xin Yu**[a], **Renita Moradian**[a], **Carson Folk**[a], **Maximilian H. Spatz**[a], **Phoebe Kim**[a], **Adil A. Bhatti**[a], **Daryl L. Davies**[a], **Jing Liang**[a,*]

[a]Titus Family Department of Clinical Pharmacy, School of Pharmacy, University of Southern California, Los Angeles, USA

Abstract

Introduction—Excess alcohol (ethanol) consumption is a significant cause of chronic liver disease, accounting for nearly half of the cirrhosis-associated deaths in the United States. Ethanol-induced liver toxicity is linked to ethanol metabolism and its associated increase in proinflammatory cytokines, oxidative stress, and the subsequent activation of Kupffer cells. Dihydromyricetin (DHM), a bioflavonoid isolated from *Hovenia dulcis*, can reduce ethanol intoxication and potentially protect against chemical-induced liver injuries. But there remains a paucity of information regarding the effects of DHM on ethanol metabolism and liver protection. As such, the current study tests the hypothesis that DHM supplementation enhances ethanol metabolism and reduces ethanol-mediated lipid dysregulation, thus promoting hepatocellular health.

Methods—The hepatoprotective effect of DHM (5 and 10 mg/kg; intraperitoneal injection) was evaluated using male C57BL/6J mice and a forced drinking *ad libitum* ethanol feeding model and HepG2/VL-17A Hepatoblastoma cell models. Ethanol-mediated lipid accumulation and DHM effects against lipid deposits were determined via H&E stains, triglyceride measurements, and intracellular lipid dyes. Protein expression of phosphorylated/total proteins and serum and hepatic cytokines were determined via Western blot and protein array. Total NAD^+/NADH Assay of liver homogenates was used to detect NAD+ levels.

Results—DHM reduced liver steatosis, liver triglycerides, and liver injury markers in mice chronically fed ethanol. DHM treatment resulted in increased activation of AMPK and downstream targets, carnitine palmitoyltransferase (CPT)-1a, and acetyl CoA carboxylase (ACC)-1. DHM induced expression of ethanol metabolizing enzymes and reduced ethanol and acetaldehyde concentrations, effects that may be partly explained by changes in NAD^+. Furthermore, DHM reduced the expression of pro-inflammatory cytokines and chemokines in sera and cell models.

*Corresponding author: Jing Liang, Titus Family Department of Clinical Pharmacy, School of Pharmacy, University of Southern California, Los Angeles, USA, Tel. 323.442.1427, jliang1@usc.edu.

Conflict of Interest

There is no conflict of interest.

Conclusion—In total, these findings support the utility of DHM as a dietary supplement to reduce ethanol-induced liver injury via changes in lipid metabolism, enhancement of ethanol metabolism and suppressing inflammation responses to promote liver health.

Keywords

Ethanol; Dihydromyricetin; Alcohol Liver Damage; Steatosis

Introduction

Alcoholic liver disease (ALD) is primarily due to ethanol-mediated injury of the liver that leads to the accumulation of fats, inflammation, and reactive oxygen species (ROS). ALD constitutes a significant public health concern in the United States, where it is estimated to affect over 14 million people (Orman, Odena and Bataller, 2013). Alcohol (ethanol)-induced fatty liver generally begins as hepatic steatosis, which is characterized by an excessive buildup of lipid droplets in hepatocytes. Over time, continued consumption of high levels of ethanol can lead to steatohepatitis and cirrhosis. The molecular mechanisms underlying the progression of ethanol-mediated disease are thought to be attributed to the combination of increased oxidative metabolites produced by the metabolism of ethanol, the inflammatory response, gut microbiota, and the increase in lipopolysaccharide, and the innate immune system (Dhanda *et al.*, 2012). Interestingly, polyphenols, the most abundant antioxidants in our daily diet, may have protective effects against ethanol-induced liver injury, possibly via anti-inflammatory and antioxidant activity. Previous investigations suggest that the chemical and biological properties of polyphenols are involved in activating mechanisms of hepato-protection against ethanol-induced oxidative damage (Ko, Chen and Ng, 2011; Tian *et al.*, 2012). Additionally, several phenolic compounds have been reported to act as anti-inflammatory agents that have indirect antioxidative activity via mechanisms of upregulating antioxidant enzymes that respond to oxidative stress (Chen and Kong, 2004).

Building evidence suggests that dihydromyricetin (DHM), a bioactive flavonoid extracted from *Hovenia dulcis*, has a broad range of beneficial properties, including antioxidant activity (Okuma *et al.*, 1995), antitumor activity, and free radical scavenging capacities which can aid in the reduction of lipid peroxidation (Jiang *et al.*, 2014; Hou *et al.*, 2015). Furthermore, there is cumulating evidence supporting the use of DHM for the treatment of alcohol use disorder (AUD) and the possible reduction/prevention of ALD in animal models. For example, Shen and colleagues found that DHM potentiates $GABA_A$ receptors and reduces the effects of ethanol on the same receptors. This activity resulted in a DHM reduction of ethanol intoxication as well as a reduction of alcohol withdrawal syndrome in rats (Shen *et al.*, 2012). DHM administration has also been found to reduce ethanol-dependent lipid accumulation in the liver via mechanisms of increased autophagy and reducing inflammatory responses, further supporting the beneficial effects of DHM on ethanol and chemical-induced outcomes (Fang *et al.*, 2007; Qiu *et al.*, 2017, 2019).

The hepatoprotective effects of DHM may be linked to its ability to protect cells against inflammatory responses and oxidative species (Hou *et al.*, 2015; Liang *et al.*, 2015). In human umbilical vein endothelial cells (HUVEC) and HepG2 hepatoblastoma (HB) cells,

DHM has been shown to reduce ROS and oxidative stress via regulatory mechanisms and its ability to scavenge radicals (Hou *et al.*, 2015; Xie *et al.*, 2016). DHM has also been shown to protect HUVECs from oxidative stress damage by altering mitochondrial apoptotic pathways involving Bcl-2, Bax, and the activation of caspase-9/caspase-3, meanwhile inducing autophagy and reducing lipid accumulation and lipogenesis *in vitro* (Hou *et al.*, 2015; Liang *et al.*, 2015; Xie *et al.*, 2016). The proposed protective effects of DHM have also been attributed to its electrophilic properties and dissociation of Nrf2 from Keap1, thereby promoting the expression and activity of antioxidant mechanisms (Qiu *et al.*, 2017; Chu *et al.*, 2018). Collectively, these data support the development of DHM as a dietary supplement to help reduce the consequences of oxidative stress and lipid metabolism and to promote liver health. However, the liver-protective mechanisms of DHM are still not well understood. In addition, much of the earlier findings were based on findings from HepG2 HB cell lines that lack enzymes capable of oxidatively metabolizing ethanol. The current study tests the hypothesis that DHM supplementation enhances ethanol metabolism and reduces ethanol-mediated lipid dysregulation, thus promoting hepatocellular health. This was accomplished by investigating the molecular mechanisms related to DHM activity using ethanol-exposed HB cells capable of oxidatively metabolizing ethanol, and an *in vivo* forced drinking mouse model to evaluate the intracellular mechanisms that contribute to hepatoprotection.

Materials and Methods

Chemicals and Reagents

DHM: [(2R, 3R)-3, 5, 7-trihydroxy-2-(3, 4, 5-trihydroxyphenyl)-2,3-dihydrochromen-4-one], MW 320.25, HPLC grade, >98% (Master Herbs Inc., Pomona, CA) was used in this study. Penicillin-streptomycin, fetal bovine serum (FBS), minimum essential medium (MEM), phosphate-buffered saline (PBS), and Dulbecco's Phosphate-Buffered Saline and Tween 20 were purchased from ThermoFisher (Life Technologies, Foster City, CA). Dimethyl sulfoxide (DMSO) and 200 proof pure ethyl alcohol were purchased from Sigma-Aldrich (St. Louis, MO).

Animals and Experimental Design

Thirty-two 6-week old male C57Bl/6J mice were purchased from Jackson Laboratories (Bar Harbor, ME). Mice were housed in temperature, light, and humidity-controlled conditions with a 12-h light/dark cycle. The mice were randomized into four groups and acclimated by single housing for one week prior to one week of daily injections of DHM (5 mg/kg or 10 mg/kg) or saline before the start of the experiment. Doses of DHM (5 and 10 mg/kg) were selected based on previous studies that identified beneficial effects of 10 mg/kg (i.p.) against dopaminergic injury, with the addition of 5 mg/kg to evaluate the potential for a lower dose in hepatoprotection (Ren *et al.*, 2016). The groups were organized as follows: 1) Water-fed + daily saline intraperitoneal (i.p). injections (n=6), 2) EtOH-fed + daily saline i.p. injections (n=6), 3) EtOH-fed + daily DHM i.p. injections (5 mg/kg; n=10), and 4) EtOH-fed + daily DHM i.p. injections (10 mg/kg; n=10). Following a forced drinking *ad libitum* feeding protocol (Tsukamoto, Matsuoka and French, 1990; Keegan, Martini and Batey, 1995; Brandon-Warner *et al.*, 2012),mice were provided single bottle access to ethanol, gradually

increasing the percentage of ethanol from 5 – 10%, then 20% every 4 days until reaching 30% ethanol (day 13 thru day 56). Mice were maintained on 30% ethanol single bottle access every day for 6 weeks after the two-week period of gradually increasing the ethanol concentration provided. Throughout the study, mice were administered DHM or saline 5 days a week via i.p. injection. Mice in the DHM group received either 5 mg/kg or 10 mg/kg of DHM throughout the entire study. Simultaneously, mice in the control groups were provided equivalent volumes of saline control via i.p. injection and provided either water (control groups) or the equivalent concentrations of ethanol throughout the study. All ethanol containing bottles were replaced with fresh ethanol every day to ensure high concentrations of ethanol by volume. All experimental procedures were approved by the USC IACUC committee, and all methods were carried out in accordance with relevant guidelines and regulations. At the end of the experimental period, the mice were euthanized via CO2 and cervical dislocation. All organs of all mice were immediately weighed after euthanization and organ harvesting. The serum was prepared by centrifugation at 1000 × g at 4°C for 10 min and was measured immediately or stored at −20°C for subsequent biochemical detection. The livers were immediately dissected and then fixed in 10% neutral buffered formalin for histopathological examination. The remainder of the fresh liver tissue was snap-frozen in liquid nitrogen, followed by preservation at −80°C until utilized.

Determination of serum biomarkers (AST, ALT, Triglycerides, and BDNF)

The activities of alanine aminotransferase (ALT) and aspartate aminotransferase (AST) in the serum samples were measured using the Sigma ALT and AST Activity Assay Kit (St. Louis, MO) and read using the BioTek Synergy H1 Hybrid Multi-Mode Reader plate reader (BioTek, Winooski, VT). Serum triglyceride content was measured using the Cayman Chemical Triglyceride Colorimetric Assay kit (Cayman Chemical, Ann Arbor, MI). Serum BDNF was measured using the R&D Systems (Minneapolis, MN, USA) Total BDNF Quantikine ELISA Kit and following the kit protocol and guidelines for serum tissue analysis.

Determination of hepatic triglycerides

Snap frozen liver tissues were prepared according to the Cayman Chemical Triglyceride Colorimetric Assay kit protocol. In short, snap-frozen liver samples were weighed and cut out to measure a 350 mg portion. The liver sample was minced in 2 mL of the kit provided diluted NP40 substitute assay reagent containing protease inhibitor cocktail. The samples were then centrifuged at 10,000 × g for 10 minutes at 4°C, and the supernatant was stored on ice or at −80°C for longer storage. The samples were further diluted using the NP40 substitute assay reagent before running samples.

Hepatic histopathological evaluation and examination of biomarkers

Liver sections were fixed in 10% neutral buffered formalin solution for a minimum of 24h, embedded in paraffin wax, sectioned at 5-μm thickness, stained with hematoxylin-eosin (H&E) and digitally photographed with a light microscope at a total magnification of 200 X. Anti-CYP2E1 polyclonal antibody was purchased from Abcam (Cambridge, MA) and detected using an Alexa Fluor 594 secondary anti-rabbit antibody and coverslipped using

Vectashield DAPI (4′6-diamidino-2-phenylindole 2HCl, Vector Labs) DAPI mounting media for IHC detection.

Cell culture and sample treatment

The HepG2 human HB cell line was kindly provided by Dr. Bangyan L. Stiles (USC School of Pharmacy, Los Angeles, CA). VL-17A cells were kindly provided by Dr. Dahn L Clemens (University of Nebraska Medical Center and Veterans Affairs Medical Center, Nebraska USA). HepG2 cells were cultured in MEM medium with 10% FBS, 5% penicillin-streptomycin, and grown in an atmosphere containing 5% CO2 at 37°C. VL-17A cells were cultured in MEM medium with 10% FBS, 5% penicillin-streptomycin, 400 μg/ml zeocin, 400 μg/ml G418, and grown in an atmosphere containing 5% CO2 at 37°C. HepG2 cells and VL-17A cells, expressing both ADH and CYP2E1, were incubated with vehicle (0.02% DMSO), ethanol (50 mM – 200 mM EtOH), DHM (100 nM – 50 μM, dissolved in DMSO) for 2 – 72 hours or co-treated with ethanol (50 mM – 200 mM) and DHM (100 nM - 50 μM) for 2–72 hours. All cell plates cultured in ethanol conditions were replaced with fresh ethanol-containing medium daily and wrapped with parafilm to reduce ethanol and acetaldehyde evaporation and stabilize conditions of acute exposure. Similarly, naïve cells utilized as controls for these ethanol studies were also wrapped with parafilm to normalize cell plating and treatment conditions. All acetaldehyde assays and experiments were conducted at 4°C to reduce acetaldehyde evaporation and reduce variability between samples. We proceeded with subsequent experiments under this condition. The maximal concentrations of ethanol that we tested were based on previous work that identified concentrations of 50 – 100 mM ethanol as causing minor effects on HepG2 viability, and concentrations of 200 mM ethanol and above causing significant damage to cell viability (Castaneda and Kinne, 2004; Liu *et al.*, 2014; Xie *et al.*, 2016). The maximal *in vitro* concentration of DHM tested in this experiment was 50 μM, as DHM concentrations above 50 μM induces cell death in HepG2 hepatoblastoma cell lines (Liu *et al.*, 2014).

Serum ethanol and acetaldehyde measurements

Eighteen 14-week old C57BL/6J male mice (Jackson Laboratories) housed in temperature, light, and humidity-controlled conditions with a 12-h light/dark cycle were separated into three groups and administered a single injection as follows: 1) 3.5 g/kg ethanol i.p, injection 2) 3.5 g/kg ethanol + DHM (5 mg/kg) i.p. injection, and 3) 3.5 g/kg ethanol + DHM (10 mg/kg) i.p. injection (6 mice per group). Mice were administered ethanol via i.p. injection to ensure constant concentrations of ethanol in all mice for accurate comparisons between groups. All mice were euthanized via CO2 and cervical dislocation 45 minutes post-injection, and whole blood samples were collected, stored at room temperature for thirty minutes, and separated by refrigerated centrifugation for 10 minutes at 2,000 × g. All samples were stored on ice immediately after separation. Serum samples were analyzed immediately after separation using the Ethanol and Acetaldehyde Assay Kit (Megazyme, Bray, Ireland) and H1 Hybrid Multi-Mode Reader Plate (BioTek, Winooski, VT) according to the manufacturer's guidelines. All acetaldehyde measurements were conducted on ice to keep samples cold and preserve acetaldehyde concentrations in solution.

Hepatic NAD+/NADH Measurements

Total NAD^+ and NADH concentrations were measured using a BioVision NAD^+/NADH Quantification Kit. Briefly, 20 mg of liver tissue was weighed, washed in cold 1X PBS, homogenized in 400 μL of NADH/NAD extraction buffer, and centrifuged at 14000 rpm for 5 min and extracted NADH/NAD was transferred to a new tube. To decompose NAD, and measure the total NADH, an aliquot of the extracted NAD/NADH samples was heated at 60°C for 30 minutes using a water bath, and then kept on ice for immediate evaluating following the protocol guidelines.

Ethanol and Acetaldehyde Measurements

Ethanol concentration and acetaldehyde production were measured using an Ethanol and Acetaldehyde Enzyme Assay Kit (Megazyme, Bray, Ireland) in 96-well plates. Acetaldehyde ammonia trimer and ethanol were used as the standard according to the manufacturer's instructions for the acetaldehyde assay and ethanol assay, respectively. VL-17A cells and HepG2 cells were incubated with 50 mM ethanol and either 100 nM – 50 μM DHM, 0.2% DMSO, or untreated for two hours before measurements using the BioTek Synergy H1 Hybrid Multi-Mode Reader plate reader (BioTek, Winooski, VT).

Measurement of intracellular reactive oxygen species (ROS) and Cytoxicity

Intracellular ROS generation was evaluated using the cell-permeant ThermoFisher CellROX Deep Red Reagent fluorogenic probe kit. HepG2 and VL-17A cells (10×10^3 cells/well) were seeded in 96-well plates and incubated with 50 – 100 mM ethanol, DHM, and ethanol with DHM for 24 hours. After the incubation, CellROX Reagent was added to a final concentration of 5 μM to the cells and incubated for 30 minutes at 37°C. After incubation with CellROX, medium and reagent were removed, and cells were washed three times with 1X PBS and measured fluorometrically using a BioTek Synergy H1 Hybrid Multi-Mode Reader plate reader. Similar to the design of the ROS measurement assay, cytotoxicity was evaluated using the Promega Mitochondrial ToxGlo Assay kit (Southampton, UK), a cell-based assay that measures cytotoxicity via a fluorogenic peptide substrate (bis-AAF-R110) and evaluated for fluorescence according to the manufacturer's protocol 24 hours after treatment conditions.

Measurement of Intracellular Lipid Accumulation

Intracellular lipid accumulation was assessed using Cayman's Steatosis Colorimetric Assay Kit with dye extraction, according to the manufacturer's protocol. HepG2 and VL-17A cells (10×10^3 cells/well) were seeded in 96-well plates and incubated with various concentrations of ethanol, DHM, and ethanol with DHM for 72 hours. Lipid accumulation was quantified using the BioTek Synergy H1 Hybrid Multi-Mode Reader plate reader.

Immunodetection of Serum and Hepatic Cytokines

Relative levels of detected cytokines in the serum and liver of mice were measured using a cytokine array kit. Briefly, sera were collected and centrifuged (2000 × g) for 10 min. The supernatant was subjected to a cytokine array that measures 40 different mouse cytokines, chemokines, and acute-phase proteins following the manufacturer's instructions (R&D

Systems; Minneapolis, MN, USA). For liver analyses, small pieces of frozen liver samples were rinsed in ice-cold 10 mM Tris-HCL (pH 7.4) and homogenized with RIPA lysis buffer containing fresh cocktail protein inhibitors. The mixture was centrifuged at 12,000 × g for 15 min, and the supernatant was subjected to cytokine array following manufacturer guidelines. For each array, supernatants from four individual animals were pooled, and three arrays were performed per condition. Finished membranes were exposed for 10 minutes to chemiluminescent detection reagents, and the chemiluminescent signal was captured using a ChemiDoc (Bio-Rad) imaging device. Densities were measured using ImageJ, with a fixed circular area placed over the grid-identified location for each cytokine and chemokine. The p-value for the fold differences had to be ≤ 0.05. Heat maps were generated after normalization of the data of the measured densities. The normalized data were then expressed as fold changes of the control value and thus, for each cytokine, with a color gradient from low to high concentrations (green to red).

Mitochondrial Isolation

Mitochondrial from liver tissue was isolated using the Abcam Mitochondria Isolation Kit for Tissue and following the manufacturer guidelines and protocol. Briefly, liver tissue was washed with washing buffer, homogenized in isolation buffer, and centrifuged at 1000 × g for 10 min. The supernatant was centrifuged again at 12,000 × g for 15 min. Pellets (mitochondrial fraction) were washed with isolation buffer containing protease inhibitor cocktail (Calbiochem) twice and resuspended with isolation buffer with protease inhibitor cocktail. Mitochondria were then quantified by BCA assay and for protein expression using Western blot.

Protein extraction and Western blot analysis

Small pieces of frozen liver samples were rinsed in ice-cold 10 mM Tris-HCL (pH 7.4) and homogenized with RIPA lysis buffer containing fresh cocktail protein inhibitors. The mixture was centrifuged at 12,000 × g for 15 min, and the supernatant was kept as the total protein extractant at −80 °C. HepG2 and VL-17A cells (9×10^5 cells/dish) were seeded in 100 mm dishes and treated with either the indicated concentrations of ethanol, DHM, or both ethanol and DHM for 24 hours. Cell lysates were prepared using a 1% Triton-X 100 lysis buffer containing protease and phosphatase inhibitors (Calbiochem). Cell extracts were quantified using the BCA Protein Assay kit (Pierce Biotechnology, Rockford, IL) according to the manufacturer's instructions. 50 μg of proteins were separated on a 4 – 20% sodium dodecyl sulfate polyacrylamide gel electrophoresis and transferred to PVDF membranes for Western blot analysis (Bio-Rad Laboratories, Hercules, CA). Transferred membrane was blocked with blocking buffer containing 5% skim milk (Bio-Rad) in 1X Tris-buffered saline with Tween 20 (Thermofisher) for 1 hour and then incubated with primary antibodies (p-AMPK, AMPK, ADH1, ALDH1A1, ALDH2 Nrf2, HO-1,p-ACC1, total ACC1, CPT1a, SREBP1, TNF-α, 4-HNE, VDAC, and IL-8) at appropriate dilutions in 1X TBST overnight at 4°C. The membrane washed three times with 1X TBST for 10 minutes and incubated with secondary antibody in 1X TBST for 1 hour, and the images were visualized with enhanced chemiluminescence detection reagent and Chemi-Doc (Bio-Rad) imaging device. Anti-IL8 and anti-SREBP1 monoclonal antibodies were purchased from Santa Cruz Biotechnology (Santa Cruz, CA). All other primary and secondary antibodies were purchased from Cell

Signaling (Beverly, MA). All trials were repeated in triplicates to confirm changes in protein expression. Densitometry analysis was performed using the ImageJ Gel Analysis Tool and normalized against untreated controls.

Data Analysis

All cellular experiments were performed in triplicates. Animal biochemical analyses were conducted using 6 – 8 separate samples from mice groups, or 4 separate samples for control groups. The data are presented as mean ± standard deviation. Statistical analysis included 2-way analysis of variance followed by Bonferroni multiple comparison test using Prism 6 (GraphPad Software, Inc., La Jolla, CA). Differences among groups were stated to be statistically significant when $p \leq 0.05$.

Results

DHM reduces ethanol-induced liver steatosis and triglyceride accumulation in the liver

DHM Attenuates Ethanol-Induced Liver Steatosis and Triglyceride Accumulation in the Liver—All ethanol-fed mice consumed an average of 39.43 g/kg of ethanol a day (Data S1A), with no significant differences in ethanol intake, total fluid intake, food intake, or bodyweight between all groups (Data S1). H&E staining results of mice chronically fed ethanol showed that ethanol-induced hepatic lipid dysregulation based on the observation of swollen hepatocytes, hepatic microvascular congestion, and macrosteatosis (Figure 1A). DHM was found to significantly reduce liver histopathological changes induced by chronic ethanol consumption (Figure 1A; 5 and 10 mg/kg DHM). Additionally, the administration of DHM (10 mg/kg) significantly reduced the ethanol-induced changes in liver mass (Fig 1B; $p<0.01$; n=8) and hepatic triglyceride content (Fig 1C; $p<0.01$; n=8). Furthermore, DHM administration significantly reduced triglyceride levels found in serum (Fig 1D; 5 mg/kg $p<0.05$ and 10 mg/kg $p<0.01$; n=8).

DHM reduces ethanol-induced intracellular lipid accumulation and mature SREBP-1 expression in vitro

***DHM reduces the expression of the lipogenic transcription factor*, sterol regulatory element-binding protein (*SREBP)-1*.—**HepG2 and VL-17A cells cultured in 50 – 200 mM ethanol for 24 hours resulted in a marked increase in the expression of mature SREBP-1 relative to the untreated samples. With the treatment of DHM, there was a significant reduction in the expression of the mature SREBP-1 protein during the 24-hour ethanol treatment period in HepG2 and VL17-A cells (Fig 2A & Data S2A; **$p<0.001$; n=3).

DHM significantly reduces lipid accumulation in HepG2 and VL-17A in vitro models—HepG2 and VL-17A cells cultured in either 50 or 100 mM ethanol for 72 hours resulted in a significant increase in intracellular lipids (Data S2B; ***$p<0.01$). Treatment with DHM significantly decreased intracellular lipid accumulation in both HepG2 and VL-17A cells (Data S2B; *$p<0.05$ and **$p<0.01$, respectively). To further assess these changes, Nile Red staining of HepG2 and VL-17A cells in either 50 or 100 mM ethanol and DHM were

imaged. As presented, 50 and 100 mM ethanol resulted in much higher lipid stained droplets (red) than the DHM (5 μM) co-treated counterpart in both HepG2 and VL-17A (Data S2C).

Furthermore, HepG2 and VL-17A cells showed significant accumulation of lipids in 50 and 100 mM ethanol co-treated with free fatty acids (FFAs) when compared against controls treated with FFA but no ethanol (Fig 2B; $^{**}p<0.01$). With 5 μM DHM co-treatment in 50 and 100 mM ethanol, both cell lines showed a significant reduction in lipid accumulation when incubated with FFAs (Fig 2B; $^{**}p<0.01$) with a dose-dependent effect observed in HepG2 cells.

DHM administration results in the activation of AMPK and the inhibition of downstream lipid processes—To identify DHM pharmacological mechanisms, we evaluated the activation state of adenosine monophosphate-activated protein kinase (AMPK), via phosphorylation at threonine (Thr)-172, and its downstream pathway involved in inhibiting FFA synthesis and activating lipid transport. In male C57BL/6J mice administered DHM for nine weeks, we found that the phosphorylation of AMPK at Thr172 was significantly increased relative to total AMPK expression in the liver (Fig 3 & Data S3; $^{*}p<0.05$; n=3/group). Direct phosphorylation of acetyl CoA carboxylase 1 (ACC1) at the serine 79 (Ser79) residue by activated AMPK was also significantly increased with DHM administration, suggesting that the increased activation of AMPK results in the direct inhibition of ACC1, thereby resulting in reduced FFA synthesis (p-ACC1; $^{*}p<0.05$ and $^{**}p<0.01$; n=3). Furthermore, the administration of DHM resulted in significantly higher expression of carnitine palmitoyltransferase-1 (CPT1a), a mitochondrial outer membrane protein regulated by AMPK that translocates long-chain fatty acids across the membrane (Fig 3 & Data S3; $^{**}p<0.01$; n=3). Collectively, these data suggest that DHM activates AMPK via phosphorylation at the Thr172 site and results in lipid metabolic responses that inhibit FFA synthesis and increases fatty acid translocation to the mitochondria for lipid oxidation.

DHM attenuated the ethanol-induced hepatic enzyme release and expression of pro-inflammatory cytokines

Serum Markers of Liver Injury and Circulating Cytokines—Mice chronically fed ethanol had a significantly higher level of AST and ALT activity in serum relative to water controls, suggesting liver injury (Fig 4A; $^{**}p<0.01$; n=6/group). Administration of DHM at 5 and 10 mg/kg significantly reduced the measured activity of serum ALT and AST in ethanol-fed mice (Fig 4A; $^{**}p<0.01$; n=6/group).

To assess the extent of ethanol-mediated injury, we evaluated the expression of cytokines circulating in the sera of C57BL/6J mice. Interestingly, we found that markers of pro-inflammatory cytokines TNF-α, interleukin (IL)-1α, interferon (IFN)-γ, TIMP metallopeptidase inhibitor 1 (TIMP1), and macrophage colony-stimulating factor (M-CSF) were reduced dose-dependently with DHM treatment (Fig 4C; $^{*}p<0.05$; n=4). Likewise, a reduction in chemokines such as CXCL2, CCL9, CCL1, and levels of the circulating endothelial cell/leukocyte adhesion molecule, intercellular adhesion molecule-1 (ICAM-1)/CD54 were reduced with treatment of DHM. Therefore, the reduction in circulatory

cytokines and chemokines involved in the activation of pro-inflammatory activation are reduced with administration of DHM in a dose-dependent response (Fig 4B; *p<0.05; n=4/group).

Hepatic Markers of Liver Injury and Inflammation—Protein expression of TNF-α was significantly elevated in mice chronically fed ethanol for 8 weeks relative to water controls (Fig 4C & Data S4A; **p<0.01; n = 3). However, when ethanol-fed mice were administered DHM at both 5 and 10 mg/kg, we observed a significant reduction in the protein expression of hepatic TNF- α (Fig 4C & Data S4C; **p<0.01; n=3).

Using a cytokine protein array, we found that ethanol-fed mice showed significant elevations of hepatic CCL21, CCL6, ICAM, endostatin, IGFBP-2 complement component 5a (C5a), C-reactive protein (CRP), and dipeptidyl peptidase (DPP)-4 (Fig 4D). Similar to our findings in serum, we observed a DHM-dependent decrease in hepatic cytokines, chemokines, and proinflammatory mediators, including IFN-γ, CCL21, DPP-4, CRP, and C5a.

DHM Ameliorates Ethanol-Mediated Reductions of serum BDNF

To further understand the extent of DHM-mediated anti-inflammatory benefits (Fig 4 & Data S2), we investigated the changes in BDNF levels in mice sera. As illustrated in Fig. 4E, chronic ethanol feeding resulted in a significant reduction of serum BDNF (*p<0.05; n = 6/group). Furthermore, we found that DHM administration at both 5 and 10 mg/kg reversed the ethanol-mediated reduction of serum BDNF (Fig 4E; *p<0.05; n = 6/group).

DHM Directly Suppresses the Ethanol Mediated Intracellular Expression of Inflammatory Markers, Activated Caspase-3, and cytotoxicity using in vitro models

Through a series of *in vitro* investigations, we analyzed the isolated effects of DHM treatment on ethanol-mediated hepatocellular expression of proinflammatory cytokines, interleukin (IL)-8, and TNF – α, by Western blot. Additionally, the pro-apoptotic marker, cleaved caspase-3, was evaluated in both cell lines. As illustrated in Data S4B, we found an ethanol-dependent increase in TNF-α, IL-8, and a dose-dependent increase in the protein expression of cleaved caspase-3 (Data S4B). DHM treatment (5 μM) resulted in significant reductions in the expression of these markers. Furthermore, we found a significantly higher magnitude of cell death associated with 100 mM ethanol in comparison to 50 mM (Data S4C; *p<0.05), and these effects were ameliorated with DHM treatment.

DHM significantly enhanced the activity and expression of alcohol dehydrogenase (ADH) and aldehyde dehydrogenase (ALDH) in isolated HB cell models and in vivo

DHM effects on ethanol metabolism were measured in both HepG2 and VL-17A cells (Data S5). DHM was tested at concentrations ranging from 0.1 μM to a maximum of 50 μM. We found a significant reduction in both ethanol and acetaldehyde (Data S5 A–C; *p<0.05) concentrations in both cell lines when incubated with 50 mM ethanol and DHM for two hours. Notably, 1 – 10 μM DHM significantly enhanced ethanol and acetaldehyde metabolism resulting in a reduction of measured extracellular concentrations of ethanol (Data S5B) and acetaldehyde (Data S5C; **p<0.01). Furthermore, 10 μM DHM

significantly increased the production of acetic acid in VL-17A cells relative to ethanol only controls and higher concentrations of DHM (Data S5D; *p<0.05).

DHM Reduced Blood Ethanol and Acetaldehyde Concentrations in C57BL/6J Mice Serum and Reversed Ethanol-Mediated Depletion of Nicotinamide Adenine Dinucleotide (NAD^+)—A follow-up study was conducted in 14-week old C57BL/6J mice (Fig 5A & B). Mice administered DHM simultaneously with ethanol exhibited significantly reduced ethanol and acetaldehyde concentrations relative to ethanol controls 45 minutes post injections (Fig 5A & B; *p<0.05 and **p<0.01; 2-way ANOVA).

We assessed the levels of NAD^+ relative to NADH in the liver (Fig 5C & D) in an effort to identify mechanistic information regarding DHM effects on metabolic activity. Mice administered 5 and 10 mg/kg DHM with chronic ethanol feeding showed higher NAD^+ concentrations compared to ethanol-fed and water-fed controls (Fig 5C; *p<0.05 5 and 10 mg/kg; 2-way ANOVA). Likewise, an elevated concentration of NAD^+ to NADH (NAD^+/NADH) ratio was observed in both doses of DHM, with 10 mg/kg showing a significant increase in NAD^+/NADH ratios (Fig 5D; *p<0.05 10 mg/kg; 2-way ANOVA).

DHM increases ethanol metabolizing enzyme expression in vitro and in vivo—Evaluation of DHM on the protein expression of ADH1, ALDH2, and ALDH1A1 ethanol metabolizing enzymes *in vitro* are displayed in Data S6. Interestingly, treatment of HepG2 cells with 5 μM DHM and the corresponding ethanol concentrations induced a higher expression level of both ADH1 and ALDH1A1, with ALDH1A1 expression being significantly higher (Data S6A; **p<0.01). Similarly, the treatment of DHM with ethanol incubation in VL-17A cells resulted in a significant dose-dependent expression of ALDH2 (Data S6B; *p<0.05).

We next assessed the protein expression of both ADH1 and ALDH2 ethanol metabolizing enzymes in the livers of ethanol-fed mice in comparison to those treated with DHM (Fig 5E). Similar to *in vitro* findings (Data S6), we found that DHM administration resulted in the significant elevation of both ADH1 and mitochondrial ALDH2 enzymes in the liver (Fig 5E; **p<0.01; n=4).

DHM reduces the hepatic expression of CYP2E1 in mice chronically-fed ethanol and increases the expression of Nrf2 and HO-1 antioxidant systems

DHM provided daily via i.p. injections significantly reduced the protein expression of CYP2E1 (green) throughout the liver of ethanol-fed mice relative to no treatment (Fig 6A). Furthermore, both doses of DHM administered via i.p. injection resulted in significant reductions of CYP2E1 expression (Fig 6B; *p<0.05 E + 5D; **p<0.01 E + 10D; n=4). Our data also shows that chronic ethanol feeding also resulted in a significant increase in the protein expression of *Nrf2* (Fig 6C; *p<0.05; n=3). However, the administration of DHM resulted in higher protein expression of *Nrf2* compared to ethanol controls (Fig 6C; **p<0.01; n=3), suggesting induction of *Nrf2*. When evaluating the protein expression of heme oxygenase (HO)-1, an antioxidant product of *Nrf2* activation, we found that the expression was significantly reduced in the livers of mice chronically fed ethanol (Fig 6D; **p<0.01; n=3). In contrast, administration of DHM resulted in a significant dose-dependent

increase in HO-1 production (Fig 6D; **p<0.01; n=3). Furthermore, DHM administration significantly reduced the expression of 4-HNE (Fig 6E; n=3; **p<0.01 for 5mg/kg and *p<0.05 for 10 mg/kg).

DHM suppresses ethanol-induced ROS generation in vitro

DHM Increases Expression of catalase, an antioxidant enzyme, and Reduces intracellular ROS generation.—HepG2 and VL-17A cells were evaluated for changes in catalase expression when cultured in ethanol and treated with DHM. Interestingly, we found no significant difference in catalase expression when tested with 50 and 100 mM ethanol (Fig 7A). However, exposing the cell lines to 5 μM DHM while being incubated in ethanol resulted in a significant increase in the cytosolic expression of catalase (*p<0.05).

To assess changes in ROS, we exposed HepG2 and VL-17A cells to ethanol and treated them with DHM (Fig 7B). ROS intensity was significantly increased in ethanol-treated cells suggesting a significant increase in ethanol-induced ROS generation, with CYP2E1 expressing VL-17A cells having higher ROS levels (Fig 7B; **p<0.01). Treatment with DHM for 24 hours resulted in a significant decrease in ethanol-induced ROS generation (Fig 7B; *p<0.05 *and* **p<0.01, respectively). At 100 mM ethanol, the 5 μM DHM treatment showed a greater effect in reducing ethanol-induced ROS levels in both cell lines relative to 2.5 μM (Fig 7B; **p<0.01).

Discussion

Findings from this study support the hypothesis that DHM supplementation enhances ethanol metabolism and reduces ethanol-mediated lipid dysregulation. The effects of DHM were found to pharmacologically impact several key enzymatic functions involved in lipid metabolism, anti-inflammation, ROS suppression, and ethanol metabolism. Furthermore, we unmasked several intracellular mechanisms that resulted in the hepatoprotection observed in the livers of male C57BL/6J mice chronically fed ethanol using a forced drinking *ad libitum* model. These findings were further supported by a series of *in vitro* experiments that demonstrate that HB cell models of human HepG2 and human VL-17A ethanol metabolizing cells are useful models for the study of DHM mechanisms. This latter work also provided insights regarding the beneficial effects of DHM in alleviating non-oxidative, HepG2, and oxidative, VL-17A, ethanol-mediated stress.

From our forced drinking rodent study, we found that all groups of male C57BL/6J mice consumed equal amounts of ethanol (Data S1A & B) with no significant changes in fluid intake, food intake, or % B.W. These levels of ethanol consumption were found to induce ethanol-mediated increases in steatosis, hepatic microvascular congestion, and triglyceride levels in the liver (Fig 1A & B). In contrast, daily administration of DHM significantly reversed lipid dysregulation. Therefore, the changes in lipid metabolism observed in DHM treated mice could not be attributed to a reduction in daily or weekly ethanol (g/kg) intake.

Using HepG2 and VL-17A cells, we found supporting evidence of DHM reducing ethanol-induced lipid accumulations and identified a significant reduction in the expression of SREBP-1, a transcription factor involved in fatty acid and lipid production, and FFA uptake

(Fig 2). To better elucidate this activity *in vivo*, we expanded our investigations on lipid metabolic signaling factors in the liver of ethanol-fed mice that results in the inhibition of AMPK, an energy-sensing activator of pathways that induce lipid breakdown and inhibition of lipid synthesis (García-Villafranca, Guillén and Castro, 2008; Galligan *et al.*, 2012; Zeng *et al.*, 2019). Similar to other polyphenolic compounds (Zang *et al.*, 2006), we found that DHM administration with ethanol feeding increased phosphorylation at the Thr172 site of AMPK, thereby counteracting ethanol-related inhibition of AMPK and its direct downstream products (Fig 3; Niu *et al.*, 2012). These findings demonstrate that DHM increases the activity of AMPK and its signaling/mediated effects on downstream lipid metabolic pathways that are typically suppressed with chronic ethanol feeding. In total, this work indicates that DHM administration reverses ethanol-mediated inhibition of hepatic AMPK and downstream signaling mechanisms that results in lipid accumulation and stress. This action of DHM partly explains the phenotypic reduction of lipids in the liver, and our *in vitro* findings of reduced SREBP-1 expression.

Activation of AMPK, and the associated reduction in lipid accumulation/stress, is one mechanism linked to decreases in hepatocellular stress and pro-inflammatory responses (Qiang *et al.*, 2016). In agreement with this finding, we found that DHM significantly reduced the levels of serum ALT and AST in ethanol-fed mice, markers commonly associated with liver damage. The extent of liver injury can also be evaluated by increased levels of pro-inflammatory markers such as IL-8, TNF-α, and an associated increase in susceptibility to stress over different periods of ethanol feeding or treatment (Hoek and Pastorino, 2002). We found that DHM significantly reduced ethanol-mediated inflammatory responses via reductions in circulatory cytokines and chemokines measured in serum (Fig 4B). Of these inflammatory markers, we found significant dose-dependent reductions of IFN-γ, and TIMP1, IL-1 α, CXCL9, CCL2, IL-7, which have all been associated with ALD, systemic inflammation, and fibrotic development in the liver (Das and Vasudevan, 2007; Degré *et al.*, 2012; Berres *et al.*, 2015; Chen *et al.*, 2015; Yilmaz and Eren, 2019). Furthermore, TNF - α, CCL-1, IL-13, and M-CSF were also found to be significantly reduced with DHM administration.

Likewise, a reduction of cytokines and chemokines were observed in the liver, thereby suggesting a significant effect of DHM mediating liver inflammation and alleviating ethanol-induced inflammation (Figs 4 C & D and Data S4A). For instance, the significant dose-dependent reduction of CRP in the liver suggests the hepatoprotective ability of DHM against a marker proposed for liver damage and increased risks of liver cancer (Chen *et al.*, 2015). Therefore, DHM administration effectively reduces the early stages of ALD and the potential progression to cirrhosis. Interestingly, we also found that chronic ethanol feeding induced a significant increase in the hepatic expression of DPP-4, which has been reported to promote insulin resistance and correlate with NAFLD (Baumeier *et al.*, 2017; Zheng *et al.*, 2017). Reductions in the ethanol-mediated hyperexpression of DPP-4 illustrates the ability of DHM to mediate insulin resistance associated with elevated hepatic DPP-4 and non-alcoholic fatty liver disease (NAFLD; Baumeier *et al.*, 2017). However, further evaluation is necessary to correlate this effect with ALD and chronic ethanol feeding. In support of these findings, we found that DHM reduces cytotoxicity and the expression of pro-inflammatory markers and the pro-apoptotic marker, caspase-3, *in vitro* (Data S4).

Furthermore, we assessed the serum levels of BDNF to expand our analysis of systemic benefits in relation to the anti-inflammatory properties of DHM. Serum BDNF is reduced under conditions of acute/chronic stress, including chronic alcoholic intake and chronic inflammation, and is associated with alcohol withdrawal severity and depression alcoholic patients (John MacLennan, Leea and Walker, 1995; Hensler, Ladenheim and Lyons, 2003; Huang *et al.*, 2008, 2011; Shi *et al.*, 2010; Xu *et al.*, 2010; Hilburn *et al.*, 2011). Here, we report a reversed outcome of reduced serum BDNF with chronic ethanol feeding (Fig 4E). These findings illustrate that the effects of DHM result in systemic benefits against ethanol injury. This outcome warrants further investigation into the effects of DHM on alcohol withdrawal and depression, as reduced serum BDNF levels are associated with severe alcohol withdrawal and relapse. Furthermore, the observed changes in serum BDNF may also play a role in the reported reduction of alcohol dependence (Shen *et al.*, 2012). Collectively, these findings of DHM hepatoprotection against ethanol-induced injury can open new avenues of research on mechanisms of DHM that might protect the liver and other organs against chemical stressors and diseases.

The observed hepatoprotection of DHM is likely to be contributed by several mechanisms throughout the liver tissue and cellular responses. Therefore, demonstration that DHM enhances ethanol metabolism via increased activity of ADH and ALDH sets the stage for future investigations for the development of DHM for liver protection in humans as well as a tool for the reduction of blood alcohol concentrations (BACs) that has been observed with DHM treatment in ethanol consuming murine models (Shen *et al.*, 2012; Sung *et al.*, 2012). To test this hypothesis and evaluate changes in ethanol metabolism, ethanol and acetaldehyde concentrations were measured in cell media and mice serum with simultaneous treatment of DHM and ethanol. Our current work demonstrated that DHM significantly increased ethanol and acetaldehyde metabolism in both HepG2 and VL-17A cell lines (Data S5) and that this activity may contribute to the reduced ethanol and acetaldehyde concentrations found in the sera of C57BL/6J mice administered equal doses of ethanol (Fig 5A & B). To begin to investigate mechanistic explanations for DHM's ability to metabolize ethanol, we investigated the concentrations of the NAD^+ coenzyme in the liver. The elevated levels of NAD^+ relative to control and ethanol-fed mice (Fig 5C & D), suggests that DHM modified hepatocellular bioenergetics that potentially plays a role in enhancing NAD^+-dependent ethanol metabolism and other NAD^+ dependent pathways. Although the elevated NAD^+ concentrations partially provide evidence for this DHM-mediated mechanism, future investigations need to evaluate DHM activity on other enzymatic systems such as ADH/ALDH enzymatic activity, and other critical NAD^+ dependent enzymes.

In combination with ethanol metabolizing activity, DHM administration was also found to induce ethanol/acetaldehyde metabolizing enzymes (Fig 5E & Data S6). Although evidence suggests that DHM plays a role in enhancing ethanol metabolism, the mechanisms supporting a reduction of ethanol intoxication and withdrawal behavior remain unclear. Therefore, the reported anti-alcohol effects of DHM on $GABA_A$Rs (Shen *et al.*, 2012) and our findings on DHM enhancing ethanol metabolism may partly contribute to the reduced intoxication behavior. However, the DHM-mediated activity on enzyme activity and induction warrant further investigation to elucidate the isolated or combination effects on ethanol metabolism and behavioral responses. Regardless, the increased activity of ADH and

ALDH, and induced expression, provides a novel mechanism of DHM that may contribute to systemic protection against ethanol-mediated toxicities and behavioral responses.

To investigate another potential mechanism of DHM hepatoprotection against ethanol injury, we examined the role of DHM treatment on the ROS-producing CYP2E1 enzyme, and *Nrf2* induction of antioxidant enzymes in response to ROS stress and ethanol metabolism (Gong and Cederbaum, 2006; Osna and Donohue, 2007). Chronic ethanol intake and feeding are associated with an increase in CYP2E1 expression and metabolism of ethanol, resulting in elevated ROS generation and liver injury (Leung and Nieto, 2013). We found that DHM significantly reduced the expression of CYP2E1 throughout the liver of ethanol-fed mice, and increased the expression of *Nrf2* and its downstream product, HO-1, supporting a previous investigation of DHM administered orally at 75 and 150 mg/kg (Fig 6; Qiu *et al.*, 2017). Furthermore, these effects were found to reduce 4-HNE expression in the liver, confirming reduced ROS stress in the liver (Fig 6E), data that was validated *in vitro* by the increased expression of catalase, another product of Nrf2, and reduced ROS levels (Fig 7). Therefore, this benefit of DHM administration is consistent with lower doses of DHM and provides an additional mechanism illustrating the utility of DHM in counteracting ethanol injury to the liver. Furthermore, the dual activation of both AMPK and *Nrf2* antioxidant inducing activity may explain the observed anti-inflammatory effects in hepatic tissue and *in vitro*.

In the present study, we delivered DHM via i.p. injections to increase its bioavailability rather than using gavage administration or other oral delivery methods. We recognize that i.p. delivery of DHM is not ideal, but it allowed for us to draw our first conclusions without the confound of bioflavonoid bioavailability issues. Future studies will work on enhancing methods to deliver DHM orally with the goal to maintain the beneficial effects of DHM, as identified in the present study. Consequently, recent investigations have started focusing on improving the bioavailability of DHM, but issues remain (Wang *et al.*, 2016; Xiang *et al.*, 2017; Zhao *et al.*, 2019). As such, our initial studies using i.p. delivery set the stage and benchmarks that can be used in future studies as we continue to work to advance DHM to the clinic. Additionally, due to the limitations of identifying direct effects of DHM on alcohol metabolic enzymes, future investigations should determine whether DHM is directly influencing metabolic activity or whether this is an indirect effect of DHM on cellular bioenergetics of DHM

Collectively, this extensive line of research suggests that DHM acts on multiple pathways to promote liver health and counteract ethanol injury. This work supports the use of DHM in preventing/reducing ethanol-mediated damage to the liver and the subsequent development of ALD. Overall, these findings support the hypothesis and demonstrate the potential for developing DHM as a novel treatment to help mitigate the consequences of ethanol-induced oxidative stress and lipid metabolism and to promote liver health.

Supplementary Material

Refer to Web version on PubMed Central for supplementary material.

Acknowledgments

This work was supported by funding and grants from the NIH NIAAA R01AA022448, USC GoodNeighbors Campaign, USC School of Pharmacy, American Foundation for Pharmaceutical Education (AFPE), and More Labs. We would also like to thank L. Asatryan, M. Choi, E. Cheung, A. Chang, A. Logrono, and L. Qi for their efforts and support during this project.

Abbreviations:

EtOH	ethanol
ACH	acetaldehyde
ALD	alcoholic liver disease
ROS	reactive oxygen species
ADH	alcohol dehydrogenase
ALDH	aldehyde dehydrogenase

References:

Baumeier C, Schlüter L, Saussenthaler S, Laeger T, Rödiger M, Alaze SA, Fritsche L, Häring HU, Stefan N, Fritsche A, Schwenk RW, Schürmann A, 2017 Elevated hepatic DPP4 activity promotes insulin resistance and non-alcoholic fatty liver disease. Mol. Metab 6, 1254–1263. [PubMed: 29031724]

Berres ML, Asmacher S, Lehmann J, Jansen C, Görtzen J, Klein S, Meyer C, Strunk HM, Fimmers R, Tacke F, Strassburg CP, Trautwein C, Sauerbruch T, Wasmuth HE, Trebicka J, 2015 CXCL9 is a prognostic marker in patients with liver cirrhosis receiving transjugular intrahepatic portosystemic shunt. J. Hepatol 62, 332–339. [PubMed: 25457205]

Brandon-Warner E, Schrum LW, Schmidt CM, McKillop IH, 2012 Rodent models of alcoholic liver disease: Of mice and men. Alcohol.

Castaneda F, Kinne RKH, 2004 Ethanol treatment of hepatocellular carcinoma: High potentials of low concentrations. Cancer Biol. Ther

Chen C, Kong ANT, 2004 Dietary chemopreventive compounds and ARE/EpRE signaling. Free Radic. Biol. Med

Chen W, Wang JB, Abnet CC, Dawsey SM, Fan JH, Yin LY, Yin J, Taylor PR, Qiao YL, Freedman ND, 2015 Association between C-reactive protein, incident liver cancer, and chronic liver disease mortality in the linxian nutrition intervention trials: A nested case-control study. Cancer Epidemiol. Biomarkers Prev 24, 386–392. [PubMed: 25613115]

Chu J, Wang X, Bi H, Li L, Ren M, Wang J, 2018 Dihydromyricetin relieves rheumatoid arthritis symptoms and suppresses expression of pro-inflammatory cytokines via the activation of Nrf2 pathway in rheumatoid arthritis model. Int. Immunopharmacol 59, 174–180. [PubMed: 29656207]

Das SK, Vasudevan DM, 2007 Alcohol-induced oxidative stress. Life Sci.

Degré D, Lemmers A, Gustot T, Ouziel R, Trépo E, Demetter P, Verset L, Quertinmont E, Vercruysse V, Le Moine O, Devière J, Moreno C, 2012 Hepatic expression of CCL2 in alcoholic liver disease is associated with disease severity and neutrophil infiltrates. Clin. Exp. Immunol 169, 302–310. [PubMed: 22861370]

Dhanda AD, Lee RWL, Collins PL, McCune CA, 2012 Molecular targets in the treatment of alcoholic hepatitis. World J. Gastroenterol 18, 5504–5513. [PubMed: 23112542]

Fang HL, Lin HY, Chan MC, Lin WL, Lin WC, 2007 Treatment of chronic liver injuries in mice by oral administration of ethanolic extract of the fruit of Hovenia dulcis. Am. J. Chin. Med 35, 693–703. [PubMed: 17708635]

Galligan JJ, Smathers RL, Shearn CT, Fritz KS, Backos DS, Jiang H, Franklin CC, Orlicky DJ, MacLean KN, Petersen DR, 2012. Oxidative stress and the ER stress response in a murine model for early-stage alcoholic liver disease. J. Toxicol 2012.

García-Villafranca J, Guillén A, Castro J, 2008 Ethanol consumption impairs regulation of fatty acid metabolism by decreasing the activity of AMP-activated protein kinase in rat liver. Biochimie 90, 460–466. [PubMed: 17997005]

Gong P, Cederbaum AI, 2006 Nrf2 is increased by CYP2E1 in rodent liver and HepG2 cells and protects against oxidative stress caused by CYP2E1. Hepatology 43, 144–153. [PubMed: 16374848]

Hensler JG, Ladenheim EE, Lyons WE, 2003 Ethanol consumption and serotonin-1A (5-HT1A) receptor function in heterozygous BDNF (+/−) mice. J. Neurochem 85, 1139–1147. [PubMed: 12753073]

Hilburn C, Nejtek VA, Underwood WA, Singh M, Patel G, Gangwani P, Forster MJ, 2011 Is serum brain-derived neurotrophic factor related to craving for or use of alcohol, cocaine, or methamphetamine? Neuropsychiatr. Dis. Treat 7, 357–364. [PubMed: 21792305]

Hoek JB, Pastorino JG, 2002 Ethanol, oxidative stress, and cytokine-induced liver cell injury. Alcohol 27, 63–68. [PubMed: 12062639]

Hou X, Tong Q, Wang W, Xiong W, Shi C, Fang J, 2015 Dihydromyricetin protects endothelial cells from hydrogen peroxide-induced oxidative stress damage by regulating mitochondrial pathways. Life Sci. 130, 38–46. [PubMed: 25818185]

Huang MC, Chen CH, Liu HC, Chen CC, Ho CC, Leu SJ, 2011 Differential Patterns of Serum Brain-Derived Neurotrophic Factor Levels in Alcoholic Patients With and Without Delirium Tremens During Acute Withdrawal. Alcohol. Clin. Exp. Res 35, 126–131. [PubMed: 21039634]

Huang MC, Chen Chun Hsin, Chen Chia Hui, Liu SC, Ho CJ, Shen WW, Leu SJ, 2008 Alterations of serum brain-derived neurotrophic factor levels in early alcohol withdrawal. Alcohol Alcohol. 43, 241–245. [PubMed: 18326550]

Jiang B, Le L, Pan H, Hu K, Xu L, Xiao P, 2014 Dihydromyricetin ameliorates the oxidative stress response induced by methylglyoxal via the AMPK/GLUT4 signaling pathway in PC12 cells. Brain Res. Bull 109, 117–126. [PubMed: 25451453]

John MacLennan A, Leea N, Walker DW, 1995 Chronic ethanol administration decreases brain-derived neurotrophic factor gene expression in the rat hippocampus. Neurosci. Lett 197, 105–108. [PubMed: 8552271]

Keegan A, Martini R, Batey R, 1995 Ethanol-related liver injury in the rat: a model of steatosis, inflammation and pericentral fibrosis. J. Hepatol 23, 591–600. [PubMed: 8583149]

Ko HJ, Chen JH, Ng LT, 2011 Hepatoprotection of Gentiana scabra Extract and Polyphenols in Liver of Carbon Tetrachloride- intoxicated mice. J. Environ. Pathol. Toxicol. Oncol 30, 179–187. [PubMed: 22126611]

Leung TM, Nieto N, 2013 CYP2E1 and oxidant stress in alcoholic and non-alcoholic fatty liver disease. J. Hepatol 58, 395–398. [PubMed: 22940046]

Liang X, Zhang T, Shi L, Kang C, Wan J, Zhou Y, Zhu J, Mi M, 2015 Ampelopsin protects endothelial cells from hyperglycemia-induced oxidative damage by inducing autophagy via the AMPK signaling pathway. BioFactors 41, 463–475. [PubMed: 26644014]

Liu J, Shu Y, Zhang Q, Liu B, Xia J, Qiu M, Miao H, Li M, Zhu R, 2014 Dihydromyricetin induces apoptosis and inhibits proliferation in hepatocellular carcinoma cells. Oncol. Lett 8, 1645–1651. [PubMed: 25202384]

Niu Y, Li S, Na L, Feng R, Liu L, Li Y, Sun C, 2012 Mangiferin decreases plasma free fatty acids through promoting its catabolism in liver by activation of AMPK. PLoS One 7, 1–8.

Okuma Y, Ishikawa H, Ito Y, Hayashi Y, Endo A, Watanabe T and Endo S, 1995 Effect of extracts from Hovenia dulcis Thunb. alcohol concentration in rats and men administered alcohol.

Orman ES, Odena G, Bataller R, 2013 Alcoholic liver disease: Pathogenesis, management, and novel targets for therapy. J. Gastroenterol. Hepatol 28, 77–84. [PubMed: 23855300]

Osna NA, Donohue TM, 2007 Implication of altered proteasome function in alcoholic liver injury. World J. Gastroenterol 13, 4931–4937. [PubMed: 17854134]

Qiang X, Xu L, Zhang M, Zhang P, Wang Yinhang, Wang Yongchen, Zhao Z, Chen H, Liu X, Zhang Y, 2016 Demethyleneberberine attenuates non-alcoholic fatty liver disease with activation of AMPK and inhibition of oxidative stress. Biochem. Biophys. Res. Commun 472, 603–609. [PubMed: 26970305]

Qiu P, Dong Y, Li B, Kang X. jie, Gu C, Zhu T, Luo Y. yun, Pang M. xia, Du W. feng, Ge W. hong, 2017 Dihydromyricetin modulates p62 and autophagy crosstalk with the Keap-1/Nrf2 pathway to alleviate ethanol-induced hepatic injury. Toxicol. Lett 274, 31–41. [PubMed: 28419832]

Qiu P, Dong Y, Zhu T, Luo Y. yun, Kang, Pang M. xia, Li H. zhou, Xu H, Gu C, Pan S. hua, Du W. feng, Ge W. hong, 2019 Semen hoveniae extract ameliorates alcohol-induced chronic liver damage in rats via modulation of the abnormalities of gut-liver axis. Phytomedicine 52, 40–50. [PubMed: 30599911]

Ren ZX, Zhao YF, Cao T, Zhen XC, 2016 Dihydromyricetin protects neurons in an MPTP-induced model of Parkinson's disease by suppressing glycogen synthase kinase-3 beta activity. Acta Pharmacol. Sin 37, 1315–1324. [PubMed: 27374489]

Shen Y, Lindemeyer K, Gonzalez C, Shao XM, Spigelman I, Olsen RW, Liang J, 2012 Dihydromyricetin as a novel anti-alcohol intoxication medication. J. Neurosci 32, 390–401. [PubMed: 22219299]

Shi S. Sen, Shao S. hong, Yuan B. ping, Pan F, Li ZL, 2010 Acute stress and chronic stress change brain-derived neurotrophic factor (BDNF) and tyrosine kinase-coupled receptor (TrkB) expression in both young and aged rat hippocampus. Yonsei Med. J 51, 661–671. [PubMed: 20635439]

Sung CK, Kim SM, Oh CJ, Yang SA, Han BH, Mo EK, 2012 Taraxerone enhances alcohol oxidation via increases of alcohol dehyderogenase (ADH) and acetaldehyde dehydrogenase (ALDH) activities and gene expressions. Food Chem. Toxicol 50, 2508–2514. [PubMed: 22554647]

Tian L, Shi X, Yu L, Zhu J, Ma R, Yang X, 2012 Chemical composition and hepatoprotective effects of polyphenol-rich extract from houttuynia cordata tea. J. Agric. Food Chem 60, 4641–4648. [PubMed: 22515645]

Tsukamoto H, Matsuoka M, French SW, 1990 Experimental models of hepatic fibrosis: A review. Semin. Liver Dis 10, 56–65. [PubMed: 2110685]

Wang C, Tong Q, Hou X, Hu S, Fang J, Sun CC, 2016 Enhancing Bioavailability of Dihydromyricetin through Inhibiting Precipitation of Soluble Cocrystals by a Crystallization Inhibitor. Cryst. Growth Des 16, 5030–5039.

Xiang D, Wang CG, Wang WQ, Shi CY, Xiong W, Wang MD, Fang JG, 2017 Gastrointestinal stability of dihydromyricetin, myricetin, and myricitrin: an in vitro investigation. Int. J. Food Sci. Nutr 68, 704–711. [PubMed: 28114854]

Xie C, Chen Z, Zhang C, Xu X, Jin J, Zhan W, Han T, Wang J, 2016 Dihydromyricetin ameliorates oleic acid-induced lipid accumulation in L02 and HepG2 cells by inhibiting lipogenesis and oxidative stress. Life Sci. 157, 131–139. [PubMed: 27265384]

Xu G, Jiang Y, Wei N, Zhu J, Lu T, Chen Z, Liu X, 2010. Effects of brain-derived neurotrophic factor on local inflammation in experimental stroke of rat. Mediators Inflamm. 2010.

Yilmaz Y, Eren F, 2019 Serum biomarkers of fibrosis and extracellular matrix remodeling in patients with nonalcoholic fatty liver disease: Association with liver histology. Eur. J. Gastroenterol. Hepatol 31, 43–46. [PubMed: 30134384]

Zang M, Xu S, Maitland-Toolan KA, Zuccollo A, Hou X, Jiang B, Wierzbicki M, Verbeuren TJ, Cohen RA, 2006 Polyphenols stimulate AMP-activated protein kinase, lower lipids, and inhibit accelerated atherosclerosis in diabetic LDL receptor-deficient mice. Diabetes 55, 2180–2191. [PubMed: 16873680]

Zeng H, Guo X, Zhou F, Xiao L, Liu J, Jiang C, Xing M, Yao P, 2019 Quercetin alleviates ethanol-induced liver steatosis associated with improvement of lipophagy. Food Chem. Toxicol 125, 21–28. [PubMed: 30580029]

Zhao X, Shi C, Zhou X, Lin T, Gong Y, Yin M, Fan L, Wang W, Fang J, 2019 Preparation of a nanoscale dihydromyricetin-phospholipid complex to improve the bioavailability: in vitro and in vivo evaluations. Eur. J. Pharm. Sci 138, 104994.

Zheng T, Chen B, Yang L, Hu X, Zhang X, Liu H, Qin L, 2017 Association of plasma dipeptidyl peptidase-4 activity with non-alcoholic fatty liver disease in nondiabetic Chinese population. Metabolism. 73, 125–134. [PubMed: 28637594]

A

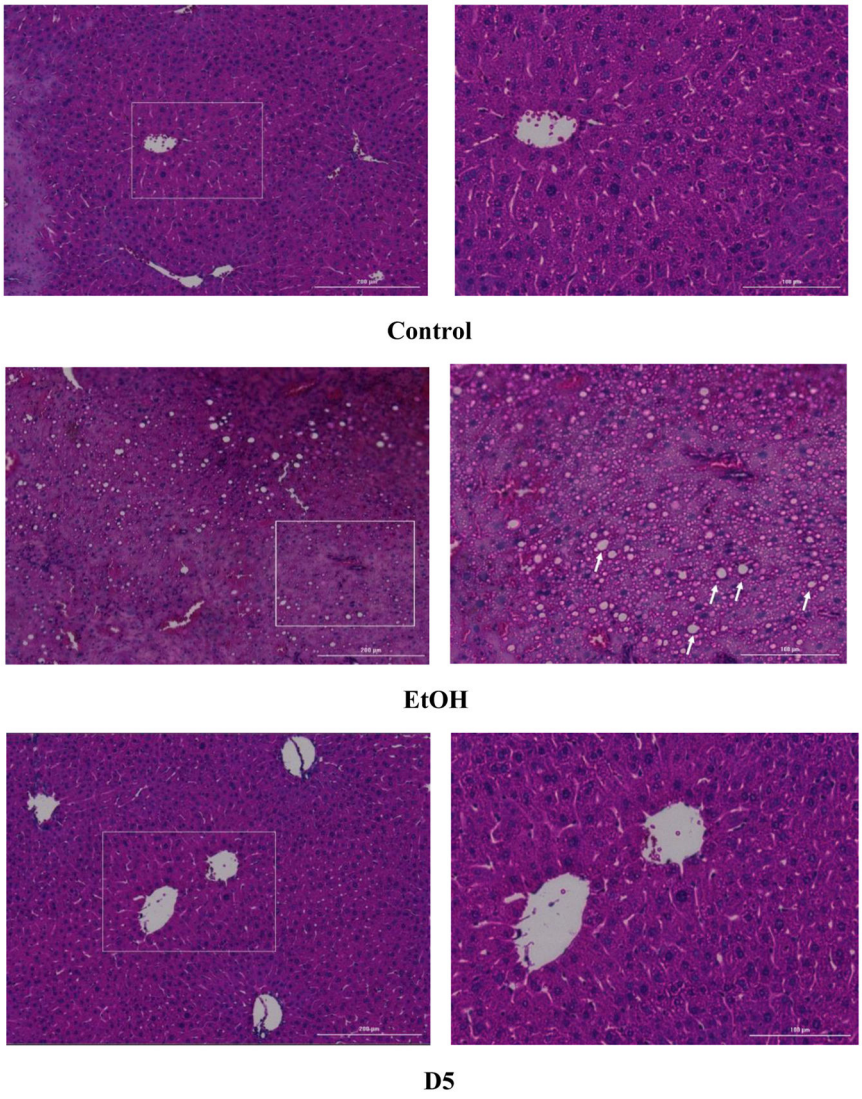

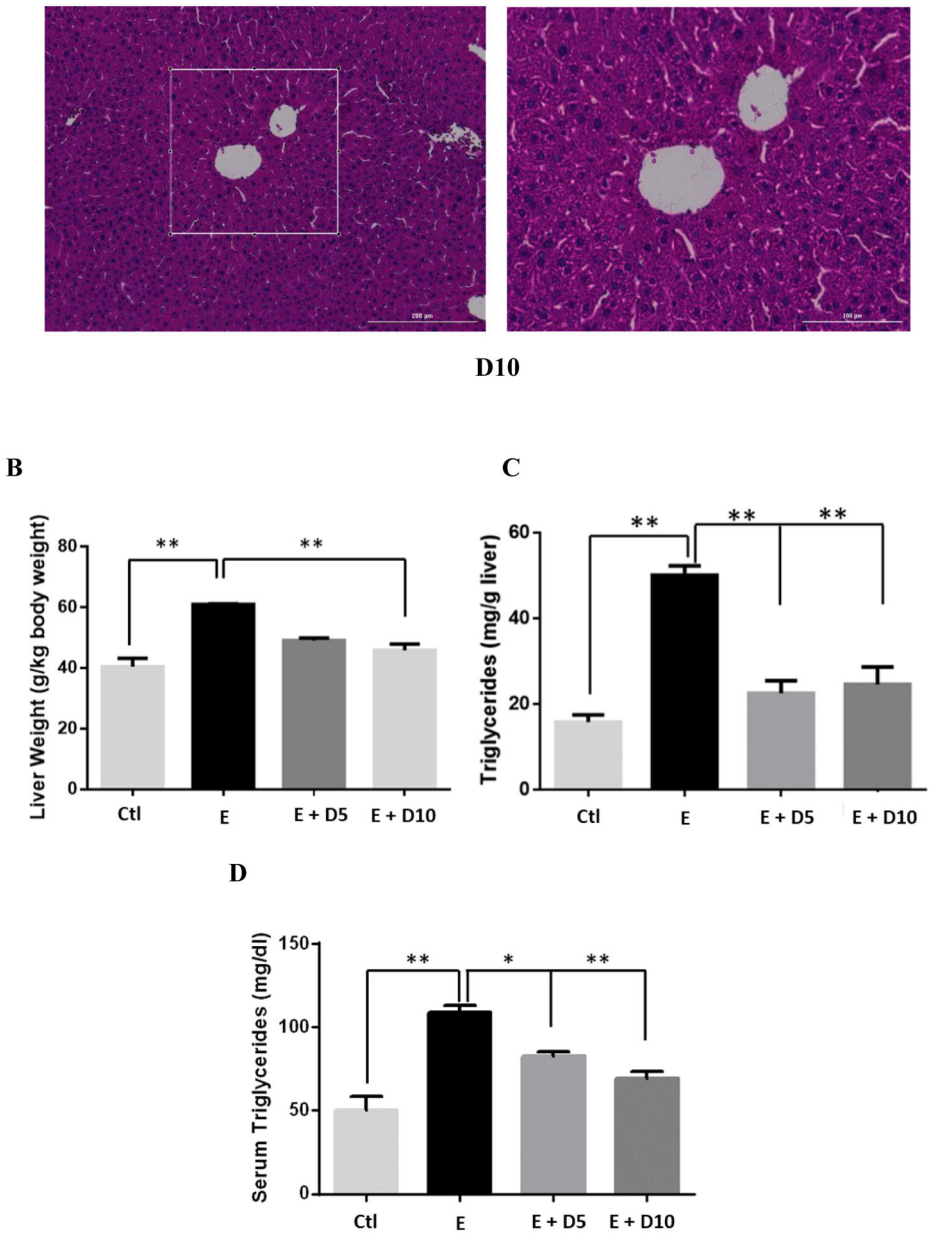

Fig 1.

DHM ameliorates ethanol-induced pathomorphology and hepatic/serum triglyceride levels in ethanol-fed mice. A) H&E (hematoxylin and eosin) staining confirmed that DHM remarkably alleviated ethanol-induced lipid deposition (white arrows). B) Ethanol-fed mice had a significantly larger liver mass compared against control (**p<0.01; n=8; 2-way ANOVA). DHM administration at 10 mg/kg significantly reduced the ethanol-mediated hepatic mass increase (**p<0.01; n.s. between DHM groups and between DHM and control; n=8; 2-way ANOVA), and C) both 5 and 10 mg/kg significantly reduced triglyceride levels in the liver (**p<0.01; n=6/group). D) Serum triglycerides were significantly elevated in ethanol-fed mice and significantly reduced in mice administered both 5 and 10 mg/kg of DHM (**p<0.01; no significant difference between 10 mg/kg DHM [E+10D] and control;

n=7; 2-way ANOVA). Data represented as mean ± SEM. p** < 0.01 compared with corresponding ethanol controls; n.s. = no significance; E = ethanol; D5 = 5 mg/kg DHM; D10 = 10 mg/kg DHM.

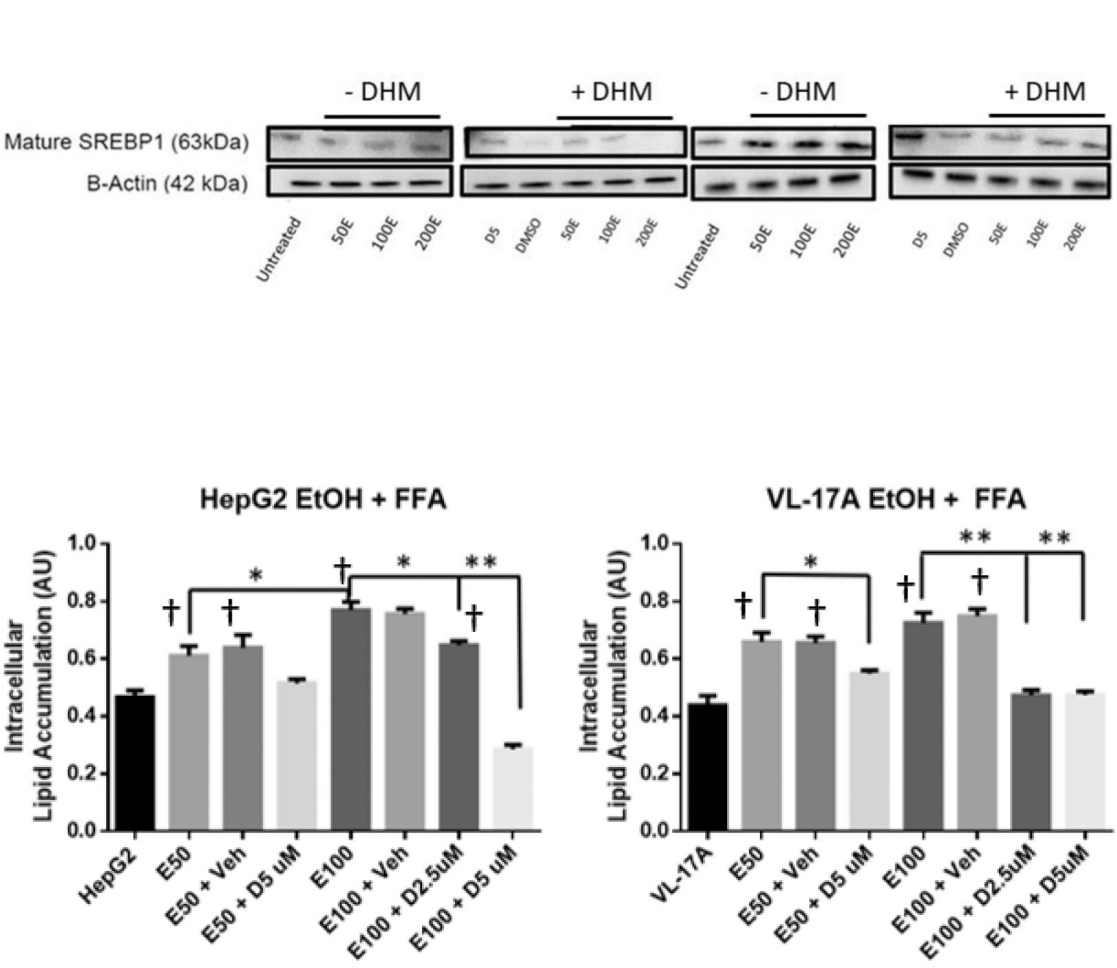

Fig 2.

DHM directly reduces ethanol-mediated mature SREBP-1 expression and lipid uptake in ethanol oxidizing (VL-17A) and non-oxidizing (HepG2) cell lines. A) Representative WB image of HepG2 and VL-17A cells cultured in EtOH and treated with 5 μM DHM or untreated for 24 hours and immunoblotted with anti-SREBP1 mAb (See Data S2A for ImageJ quantification of triplicates). B) HepG2 and VL-17A cells were cultured in 50 or 100 mM EtOH + 4 mM free fatty acids (2:1 Oleic to Palmitic acid) and either untreated or treated with either 2.5 μM or 5 μM DHM for 72 hours before photometric detection of intracellular lipid accumulation. Data represented as mean ± SEM. *$p < 0.05$ and p** < 0.01 compared with ethanol controls. †, $p<0.05$ vs. untreated control; n=3. A.U. = arbitrary units.

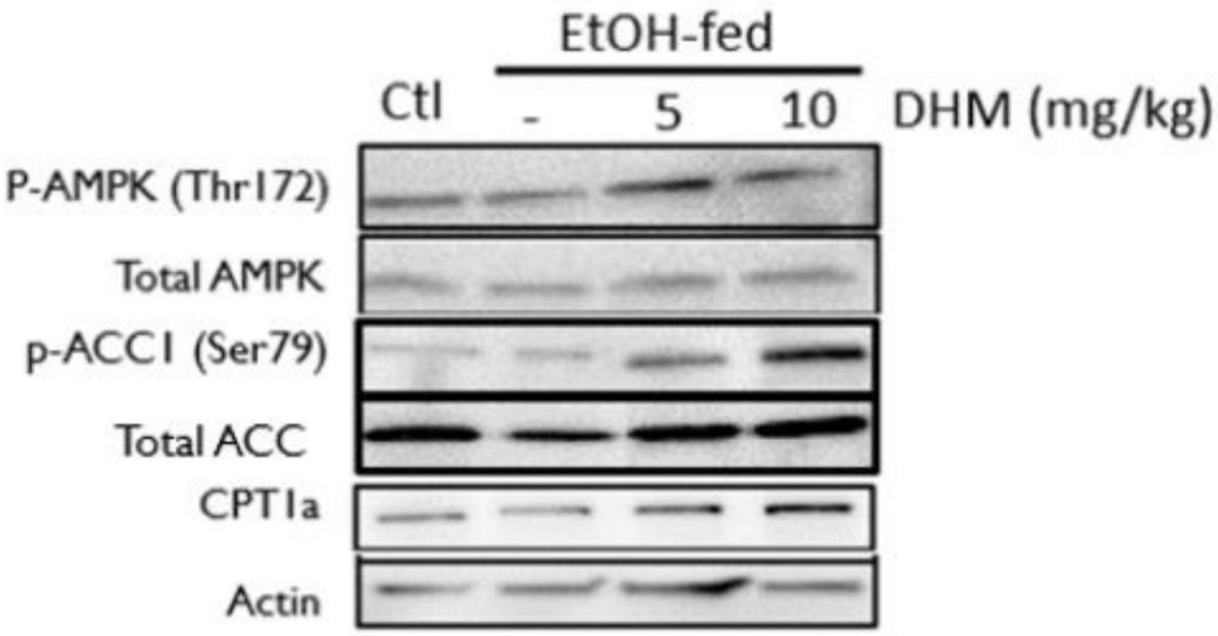

Fig 3.

DHM administration counteracts EtOH-mediated inhibition of AMPK and downstream lipid metabolic responses. Representative WB of phosphorylated AMPK (p-AMPK [Thr172]), total AMPK, phosphorylated ACC1 (p-ACC1 [Ser79]), total ACC1, total CPT1a, and β-actin loading control. EtOH-fed mice showed a significant reduction in p-AMPK (Thr172) and increase in p-ACC1 (Ser79) relative to water-fed controls (Ctl). DHM administration at both 5 and 10 mg/kg resulted in a significant increase in p-AMPK (Thr172), CPT1a expression, and a significant reduction in p-ACC1 (Ser79) relative to EtOH-fed mice and water-fed mice (Ctl). The Western blot images are representative of Western blots obtained from 3 different biological experiments. n=3/group. See Data S3 for Image J quantification of triplicates.

A

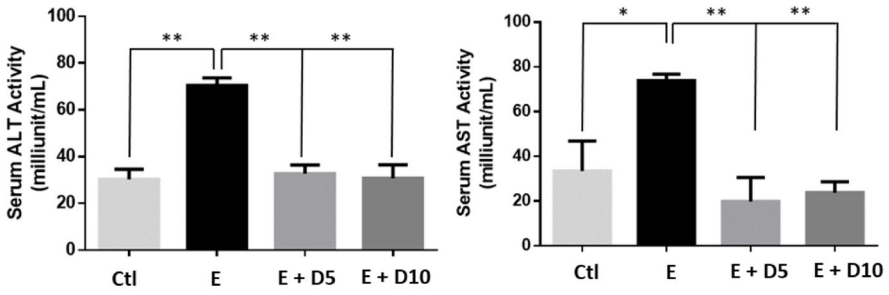

B

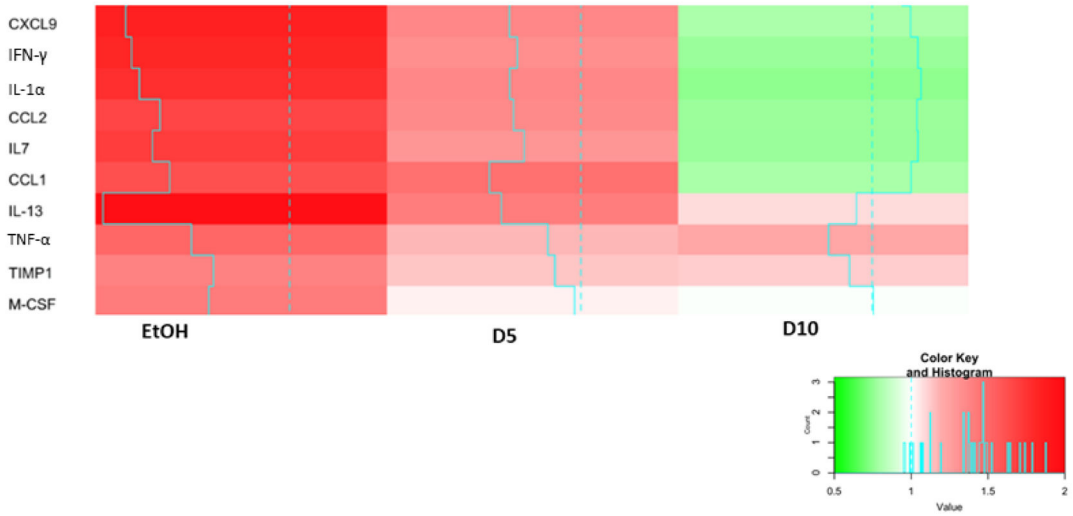

C

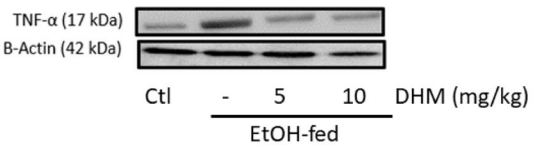

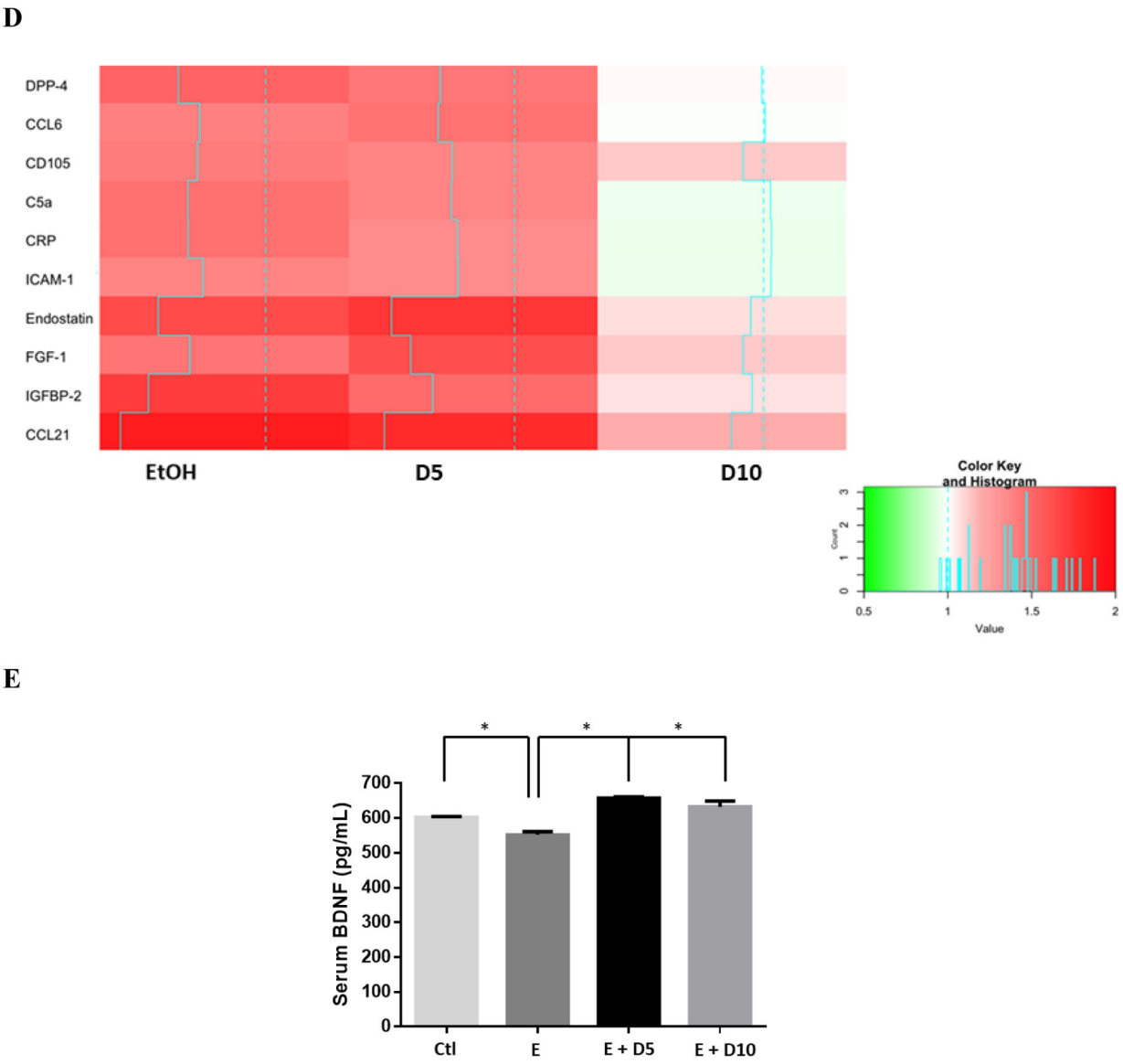

Fig 4.

DHM significantly reduces hepatic enzyme release, exhibits dose-dependent anti-inflammatory actions, and maintains serum BDNF levels. A) DHM administration at both 5 and 10 mg/kg significantly inhibited the activities of serum ALT and AST comparable to control values (n=6/group). B) DHM dose-dependently decreased serum cytokine markers compared to untreated ethanol-fed mice serum (n=4/group). C) DHM administration, at both 5 and 10 mg/kg, significantly reduced ethanol-mediated hepatic TNF-α expression relative to ethanol only controls (n=3/group; See Data S4A for Image J quantification of triplicates). D) Hepatic cytokine analysis of mice chronically-fed EtOH and either treated with DHM (5 or 10 mg/kg) or untreated (n=4/group). E) DHM administration at both 5 and 10 mg/kg significantly reversed ethanol-mediated reductions in serum BDNF concentrations (n=6/group). Color key and histogram illustrate the intensity of red being associated with larger fold increases in expression relative to normalized control values (white), and intense greens

are associated with fold-decreases (0.5-fold the lowest) relative to normalized control values. Blue solid lines indicate average fold values relative to control (dotted blue line). Data represented as mean ± SEM. *p<0.05 compared with corresponding ethanol controls. *p<0.05 and **p < 0.01 compared with corresponding ethanol controls. E = ethanol; D5 = 5 mg/kg DHM; D10 = 10 mg/kg DHM.

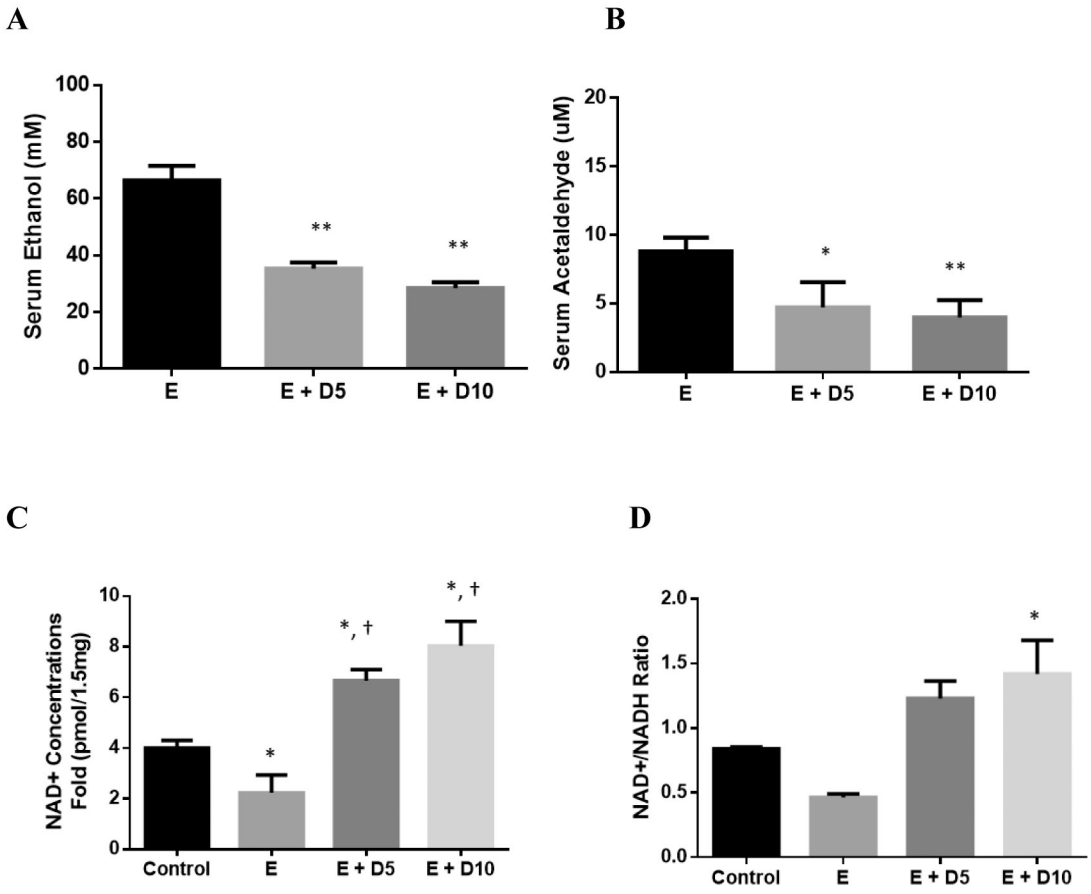

E

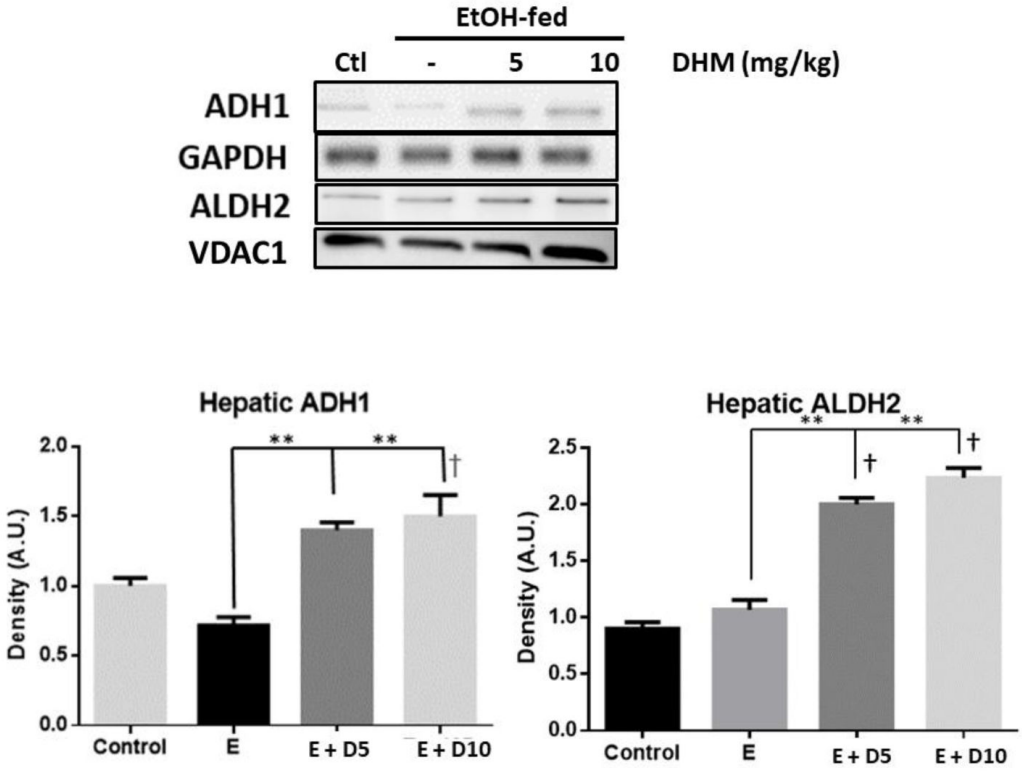

Fig 5.

DHM reduces serum ethanol and acetaldehyde concentrations in mice administered 3.5g/kg ethanol, reverses chronic ethanol-mediation depletion of hepatic NAD^+ levels, and induces hepatic ADH1/ALDH2. Serum A) ethanol and B) acetaldehyde concentration differences measured in 16-week old mice injected with 3.5 g/kg ethanol and DHM (5 or 10 mg/kg) 45 minutes after injections (*p<0.05 and **p<0.01; n=6/group, 2-way ANOVA). C) Mice chronically fed ethanol for 8-weeks show significantly less NAD^+ concentrations in the liver than water-fed controls (*p<0.05; n=6/group; 2-way ANOVA). Mice administered DHM at both 5 and 10 mg/kg showed elevated NAD^+ concentrations relative to ethanol-fed controls and water-fed controls (*p<0.05, compared to ethanol controls and †, *p<0.05, compared to water-fed controls). D) Hepatic NAD^+/NADH ratio showing a significant increase in the ratio of mice treated with 10 mg/kg DHM (*p<0.05). E) Representative Western blot images of hepatic expression of ADH1 and ALDH2 in C57BL/6J mice chronically fed ethanol and either treated with or without DHM. Data represented as mean ± SEM. E = ethanol, D5 = 5 mg/kg DHM, and D10 = 10 mg/kg DHM.

A

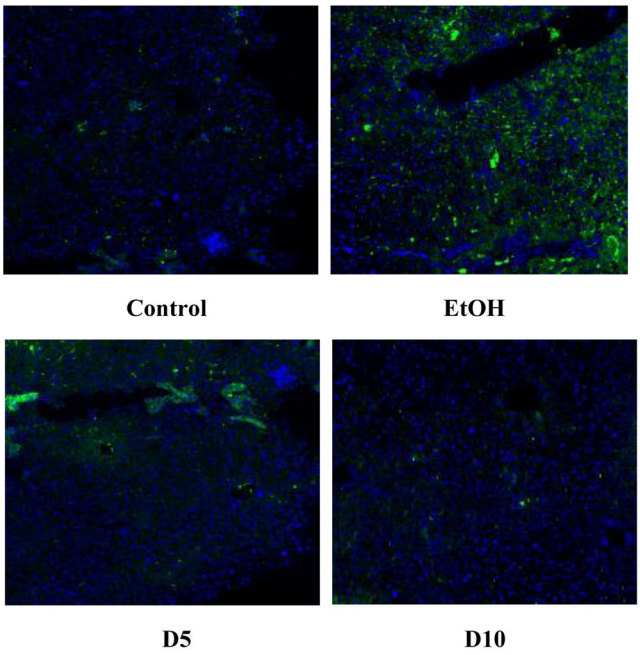

B

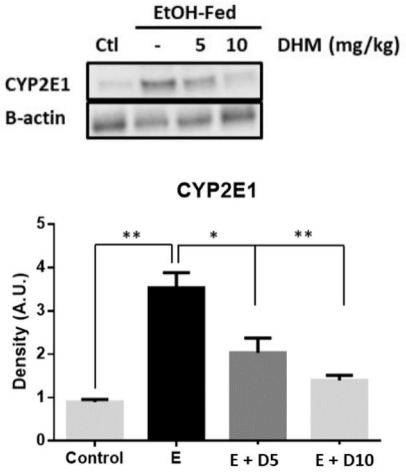

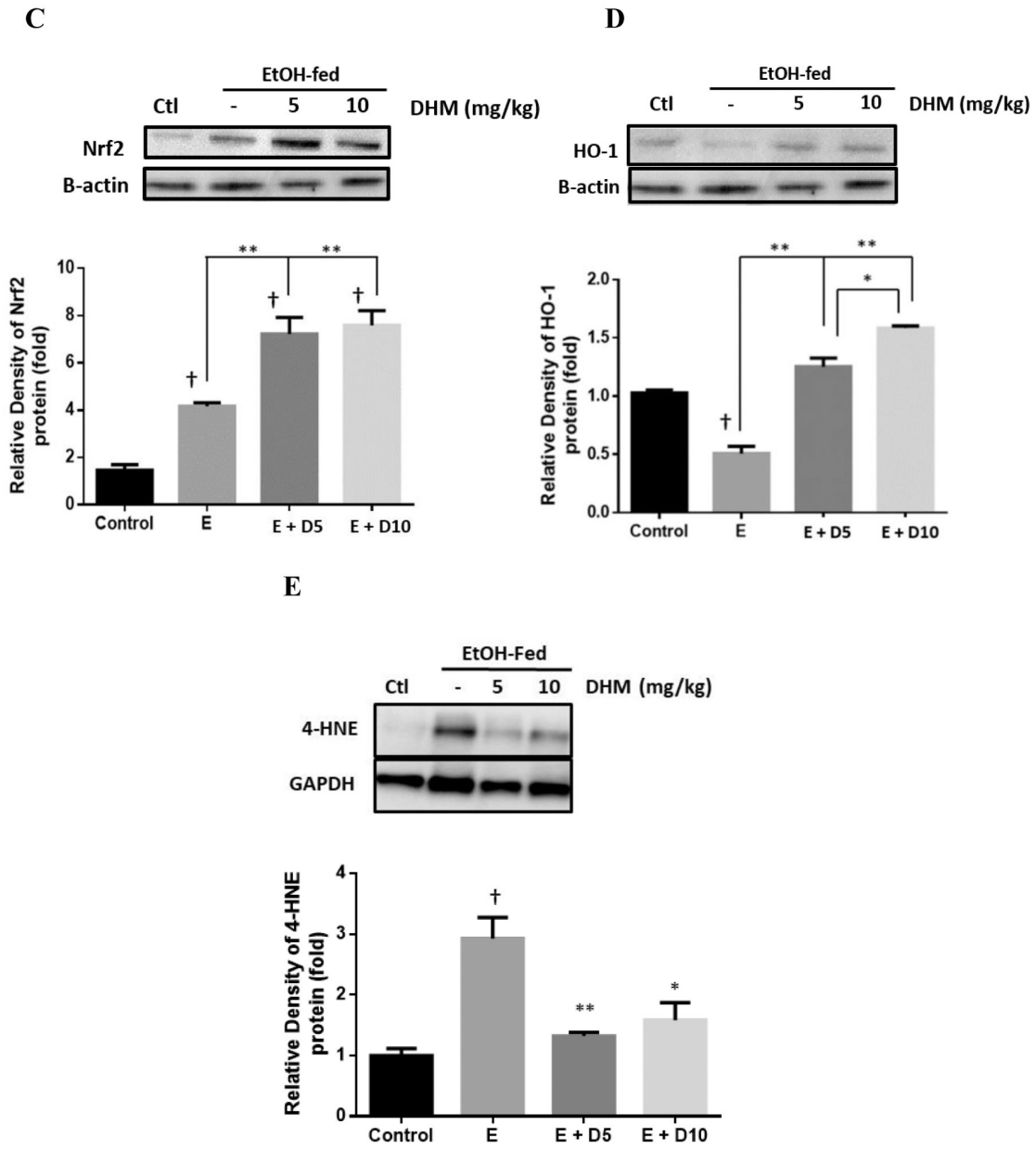

Fig 6.

DHM reduces hepatic CYP2E1 expression and increases the hepatic expression of Nrf2 and HO-1 antioxidant pathways. A) Immunohistochemistry results of CYP2E1 in livers suggests that DHM inhibited the expression of CYP2E1 in ethanol-fed mice relative to ethanol only (green=CYP2E1, blue=nuclei; n=6/group). B) Representative Western blot illustrating that DHM significantly reduces the hepatic expression of CYP2E1 relative to untreated ethanol-fed mice (n=3/group; *p<0.05 5 mg/kg DHM and **p<0.01 10 mg/kg DHM). C) Ethanol-fed mice showed a significant increase in Nrf2 relative to water controls (n=3/group; *p<0.05). DHM (5 and 10 mg/kg) significantly increased the expression of Nrf2 in ethanol-fed mice livers relative to ethanol controls (n=3/group; **p<0.01). D) Ethanol-fed mice displayed a significant reduction in HO-1 protein expression relative to water controls (n=3/

group; **p<0.01). 5 and 10 mg/kg DHM significantly increased the expression of HO-1 protein expression relative to ethanol only (n=3/group; **p<0.01; significant difference between 5 and 10 mg/kg DHM, *p<0.05). E) Ethanol-fed mice showed a significant increase in the hepatic expression of 4-HNE in comparison to water-fed controls (n=3/group; †p<0.05). DHM (5 and 10 mg/kg) significantly reduced the expression of 4-HNE in the liver (n=3/group; **p<0.01 and *p<0.05, respectively). Bar graphs were generated by quantifying blots from three independent experiments using ImageJ and normalized against intensity of the untreated lane. Data represented as mean ± SEM. *p < 0.05 and p** < 0.01 compared with corresponding ethanol controls; †, p<0.05 vs. water-fed control. n=3/group.

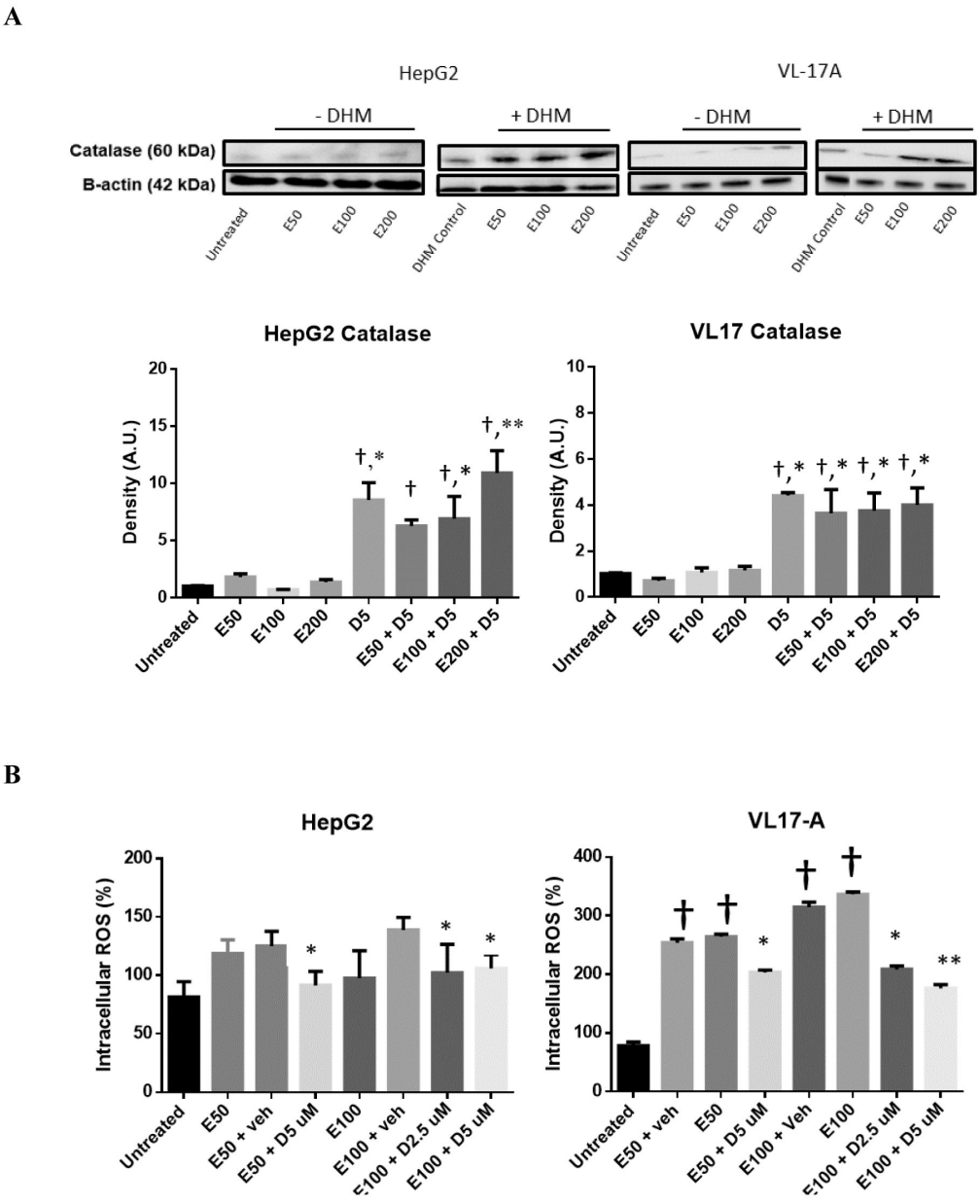

Fig 7.

DHM increases the expression of catalase and suppresses ethanol-mediated ROS generation *in vitro*. A) Representative Western blot image of HepG2 and VL-17A cells cultured in ethanol and either 5 μM DHM or untreated for 24 hours and immunoblotted with anti-Catalase mAb. B) HepG2 and VL-17A cells were cultured in 50– 100 mM ethanol and treated with 2.5 – 5 μM DHM or untreated for 24 hours before fluorometric analysis of intracellular ROS levels. Bar graphs were generated by quantifying blots from three independent experiments using ImageJ and normalized against intensity of the untreated lane. Data represented as mean ± SEM. *p < 0.05 and p** < 0.01 compared with

corresponding ethanol controls and normalized with untreated controls; †, $p<0.05$ vs. untreated control. n=3/group. ROS = reactive oxygen species. A.U. = arbitrary units.